

## Energy and massresolved detection of neutral and ion species using modulatedpolebias quadrupole mass spectroscopy

A. M. Myers, D. N. Ruzic, R. C. Powell, N. Maley, D. W. Pratt et al.

Citation: *J. Vac. Sci. Technol. A* **8**, 1668 (1990); doi: 10.1116/1.576827

View online: <http://dx.doi.org/10.1116/1.576827>

View Table of Contents: <http://avspublications.org/resource/1/JVTAD6/v8/i3>

Published by the AVS: Science & Technology of Materials, Interfaces, and Processing

### Related Articles

Focused chromium ion beam

*J. Vac. Sci. Technol. B* **28**, C6F1 (2010)

Three dimension analysis of E×B mass separator

*J. Vac. Sci. Technol. B* **25**, 194 (2007)

Focusing of MeV ion beams by means of tapered glass capillary optics

*J. Vac. Sci. Technol. A* **21**, 1671 (2003)

Characteristics of a large diameter reactive ion beam generated by an electron cyclotron resonance microwave plasma source

*J. Vac. Sci. Technol. A* **19**, 539 (2001)

Tandem accel lens advantageous in producing a small spot focused ion beam

*J. Vac. Sci. Technol. B* **17**, 82 (1999)

### Additional information on *J. Vac. Sci. Technol. A*

Journal Homepage: <http://avspublications.org/jvsta>

Journal Information: [http://avspublications.org/jvsta/about/about\\_the\\_journal](http://avspublications.org/jvsta/about/about_the_journal)

Top downloads: [http://avspublications.org/jvsta/top\\_20\\_most\\_downloaded](http://avspublications.org/jvsta/top_20_most_downloaded)

Information for Authors: [http://avspublications.org/jvsta/authors/information\\_for\\_contributors](http://avspublications.org/jvsta/authors/information_for_contributors)

## ADVERTISEMENT

# Instruments for advanced science

**Gas Analysis**



- dynamic measurement of reaction gas streams
- catalysis and thermal analysis
- molecular beam studies
- dissolved species probes
- fermentation, environmental and ecological studies

**Surface Science**



- UHV TPD
- SIMS
- end point detection in ion beam etch
- elemental imaging - surface mapping

**Plasma Diagnostics**



- plasma source characterization
- etch and deposition process reaction kinetic studies
- analysis of neutral and radical species

**Vacuum Analysis**



- partial pressure measurement and control of process gases
- reactive sputter process control
- vacuum diagnostics
- vacuum coating process monitoring

contact Hiden Analytical for further details

**HIDEN ANALYTICAL**

[info@hideninc.com](mailto:info@hideninc.com)  
[www.HidenAnalytical.com](http://www.HidenAnalytical.com)

CLICK to view our product catalogue 

# Energy and mass-resolved detection of neutral and ion species using modulated-pole-bias quadrupole mass spectroscopy

A. M. Myers, D. N. Ruzic, R. C. Powell, N. Maley, D. W. Pratt, J. E. Greene,  
and J. R. Abelson

*Department of Materials Science and the Coordinated Science Laboratory, University of Illinois, Urbana,  
Illinois 61801*

(Received 23 October 1989; accepted 1 January 1990)

An analyzer capable of determining the mass as well as the energy (5–200 eV) of neutral and ion species has been developed from a quadrupole mass spectrometer (QMS). The system, which is similar to a retarding grid energy analyzer (RGEA), functions by biasing the rods of a QMS and monitoring the analyzer signal as a function of bias potential. Modulation of the pole bias greatly increases the minimum detectable signal level. Experiments were performed using species generated in a single-grid Kaufman ion gun operated with  $N_2$  or Ar. Results show that the pole bias techniques can provide energy resolution of 1–2 eV. Ion species from the gun were found to have an energy equal to the sum of the beam and the plasma potentials, with an energy spread between 1 and 3 eV. Fast  $N_2$  and Ar neutral species were measured as a function of discharge voltage (30–80 V), beam acceleration voltage (50–100 V), grid voltage (–20 to +5 V), and pressure (0.5 and 1.5 mTorr). The energy of the fast neutral species was always less than that of the ions. This was consistent with the fast neutrals being formed by a charge-exchange process.

## I. INTRODUCTION

Plasma processes and ion-beam techniques are widely used to grow or alter a variety of thin-film materials.<sup>1</sup> The kinetic energy and composition of both the ion and neutral species impinging on a surface during processing have a significant effect on the final material properties. Energy analyzer/quadrupole mass spectrometer (QMS) combinations have been used by several authors to simultaneously determine ion species and their energy distributions.<sup>2–5</sup> A dc bias has been applied to the QMS rods (“pole bias”) to determine the kinetic energy distribution of ions produced by inductively coupled plasmas.<sup>6,7</sup> In those studies, the performance, resolution and absolute energy calibration of this system were not evaluated. Energy analysis of neutral species is more difficult, requiring instruments such as a time-of-flight spectrometer<sup>8</sup> or a cylindrical mirror analyzer coupled with a QMS.<sup>9</sup>

We have extended the pole bias energy analysis (PBEA) technique, in which a QMS behaves like a retarding grid energy analyzer (RGEA), to the study of energetic neutrals. Detection of small energetic neutral fluxes is difficult, because a large, mass-independent, background signal is produced when unionized energetic particles strike the particle detector in the QMS. The low signal-to-noise ratio can be improved two orders of magnitude by modulating the pole bias, and using lock-in amplification techniques. The present system provides both mass and energy resolution for neutral and ion species with kinetic energies between 5 and 200 eV.

The QMS with PBEA is ultrahigh vacuum (UHV) compatible and was designed so that it could be inserted in a deposition or etching chamber with the sampling orifice position located in the substrate plane. In a typical application, a series of films would be grown by a plasma or ion-beam deposition source, and the film properties measured as a function of deposition parameters. The substrate holder

would then be removed, the PBEA inserted, and the incident particle fluxes analyzed and correlated with the film properties.

In this study, the PBEA was used to evaluate the species emitted from a single-grid Kaufman ion source operated with  $N_2$ , or Ar. While ion energy distributions from Kaufman-type ion sources have been measured,<sup>10,11</sup> the fast neutral energy distributions have not been investigated from these sources. We report the ion and fast neutral energy distributions versus ion source operation conditions, the ratio of neutral and ion fluxes, and discuss the neutralization mechanism.

## II. EXPERIMENTAL PROCEDURE

The ion source used in these experiments is shown schematically in Fig. 1. It is a 3 cm hot-cathode, dc-discharge source with a diverging magnetic field. The standard two-grid extraction system has been replaced by a single, 140 mesh, 74% transmittance, tungsten grid to increase the beam current at the low energies used in these experiments. Gas enters directly into the rear of the discharge chamber. Electrons are supplied to the discharge by a cathode filament driven with an ac power supply. The discharge is maintained by a dc potential ( $V_d$ ) between the cathode filament and the discharge chamber walls, which serve as the anode. The beam extraction power supply, which maintains the entire cathode-anode assembly positive at the beam potential ( $V_b$ ) with respect to the main chamber, serves to accelerate positively charged ions. The grid bias ( $V_g$ ) was varied to study the charge-exchange neutralization process. No external filament was used to provide beam space-charge neutrality. All of the dc power supplies were confirmed to have less than 1% ripple. Figure 1 also shows the qualitative potential distribution along the ion gun axis.<sup>12</sup>

Figure 2 is a schematic diagram of the experimental sys-

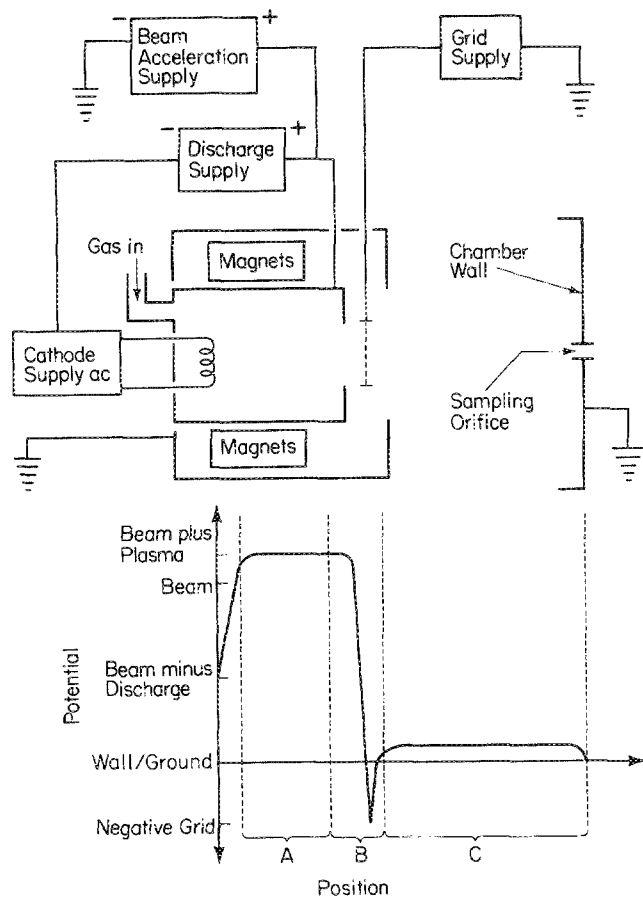
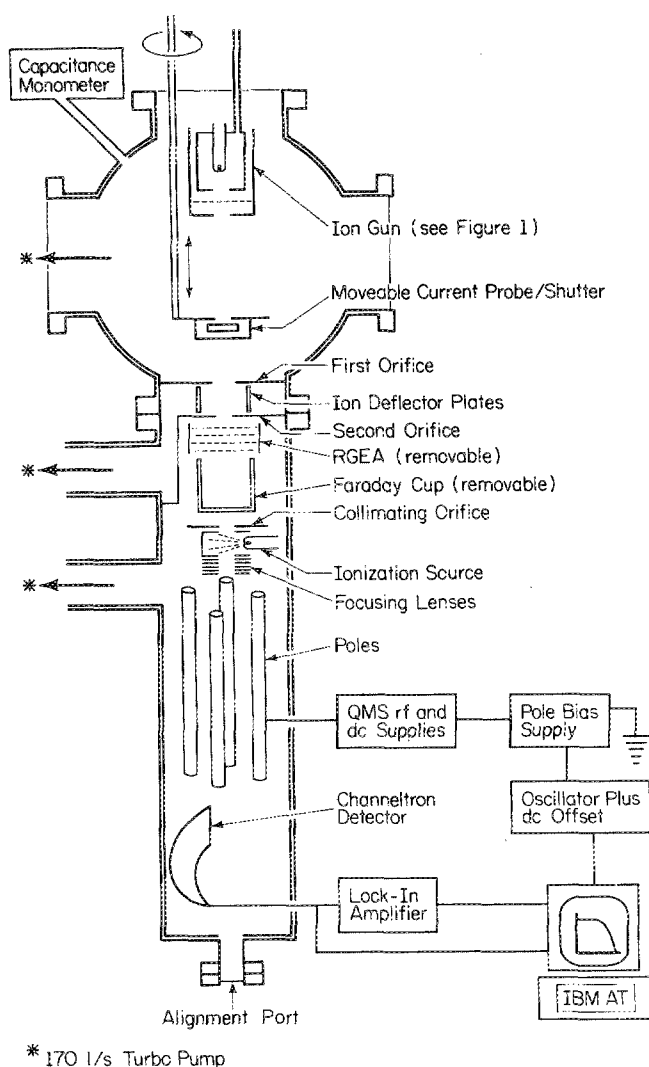


FIG. 1. A schematic diagram of the single-grid Kaufman ion source used in this experiment. The potential along the gun axis is also shown.

tem. The ion gun is mounted in an O-ring sealed chamber with a base pressure of  $1 \times 10^{-6}$  Torr. With gas flowing, the pressure is monitored using a capacitance manometer. A flat probe, electrically biased to  $-60$  V, is rotated into and translated along the beam path to measure the ion beam current density and spatial distribution. The probe also acts as a shutter for the PBEA apparatus.

The particle beam enters the PBEA through two 2 mm diam, differentially pumped, collimating orifices spaced 4 cm apart. After passing through the sampling orifice, the beam is in the molecular-flow regime, ensuring that both the identity and energy of the species are preserved. A pair of deflector plates located between the two orifices can be electrically biased to remove any charged beam components. The deflector plates also serve to quench any excited neutral species, by relaxing the selection rules for electronic deexcitation. This is important when the QMS ionization source is run in an appearance potential mode.<sup>13,14</sup> The pressure is  $5 \times 10^{-8}$  Torr between the orifices, and  $5 \times 10^{-9}$  Torr behind the second orifice where the QMS resides. All sections of the vacuum system are pumped with 170 //s turbomolecular pumps.

Upon exiting the second orifice, the beam passes through a RGEA,<sup>15,16</sup> which uses tungsten 140 mesh screens having a 74% transmittance. The entry and exit screens are at ground



\* 170 l/s Turbo Pump

FIG. 2. A schematic diagram of the experimental apparatus. The current probe/shutter, RGEA, Faraday cup, and QMS can be independently removed from the beam path.

potential. Inside the RGEA, the beam passes through a pair of screens spaced 1.6 mm apart, which are biased at  $-60$  V in order to repel any electrons. Another pair of screens, spaced 1.6 mm apart, are located 1.6 mm further down the beam path, and are biased positively with a computer-controlled variable dc power supply.

The energy distribution of ions is determined three different ways: using a RGEA/Faraday-cup combination (with no QMS) to determine the emitted species from the ion gun, using a RGEA/QMS combination to characterize the QMS response to energetic particles, and using a QMS/pole bias combination to evaluate the PBEA. The energy distribution of neutral species can only be determined with the QMS/pole bias combination. For neutral detection, the ion deflectors are biased to  $+100$  V, while the ionizer emission current is set to 10 mA with a 100 eV electron ionization energy to maximize the ionizer efficiency. When determining the neutral energy distribution, the potential that accelerates

ions into the rod system, as well as the potentials on the focusing lenses of the QMS ion source are set to zero, which avoids altering the energy of the detected particles.

### III. RESULTS AND DISCUSSION

#### A. Calibration

In order to determine the energy resolution of the PBEA, the energy distribution of ions emitted from the gun was characterized using a 2.5 cm diam, 12.5 cm long Faraday cup. This 5:1 aspect ratio helped minimize the loss of secondary electrons when energetic particles struck the back of the cup. The current from the cup was fed into a current-to-voltage amplifier with a gain of  $10^8$  V/A and then into a RC filter with a 0.5 s time constant for smoothing. Accounting for the grid transmission, we estimated that the minimum detectable ion flux was  $5 \times 10^{11}$  ions  $\text{cm}^{-2} \text{s}^{-1}$ . An example of the ion signal versus retarding potential for this technique is shown in Fig. 3. The Faraday cup/RGEA curves were fit to a quadratic spline and differentiated in order to obtain the ion energy distribution.

With the incident ion distribution determined, the Faraday cup was removed, and an Extrel C-50 QMS installed with the quadrupole rods parallel to the beam path. The known response of the RGEA was then used to evaluate the ability of the QMS to detect energetic particles. A third orifice, 1.6 mm in diameter, was placed in front of the QMS ionization source to further increase the beam collimation. The orifices and ion gun were aligned with respect to the QMS axis using a HeNe laser placed behind the quadrupole rods. In order to sample the ion flux, the deflector plates were grounded, the QMS ionization source turned off, and the charge-to-mass ratio of interest selected. Figure 3 shows

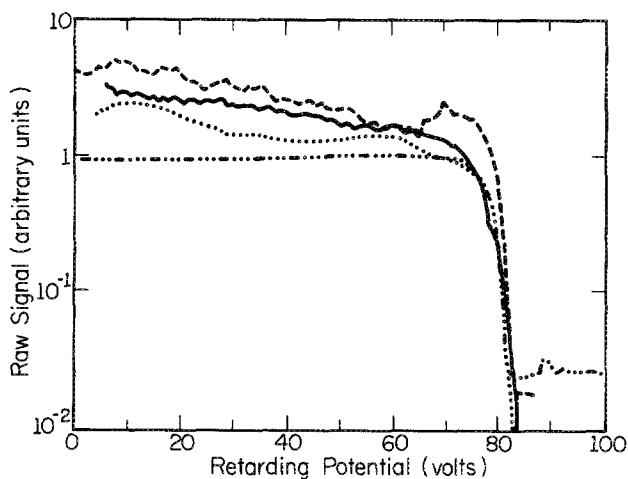


FIG. 3. The ion signal plotted in arbitrary units vs the retarding potential for  $\text{N}_2^+$  created in a  $\text{N}_2$  discharge. The magnitude of each signal relative to another is arbitrarily spread for presentation purposes. The signal shape, not the magnitude will affect the energy distribution. Pressure = 1 mTorr,  $V_{\text{beam}} = 75$  V,  $V_{\text{discharge}} = 50$  V,  $I_{\text{discharge}} = 50$  mA,  $V_{\text{grid}} = 5$  V. Faraday cup RGEA (.....), QMS/RGEA (—), QMS/dc pole bias (---), and QMS/modulated pole bias (-·-·).

that the results from both the QMS and the Faraday cup, acting as ion detectors, agree closely near the cutoff.

The RGEA was removed in order to evaluate the PBEA. This increased the particle flux into the QMS. The PBEA could be operated in both dc and ac modes. During dc operation, the quadrupole rods were biased with respect to ground and, as a consequence, with respect to the QMS ionization source. The pole bias was varied between 0 and 200 V. However, as the bias approached 200 V, the QMS resolution deteriorated. A typical result of ion energy analysis using the dc method is shown in Fig. 3, indicating the cut-off edge to be in close agreement with the Faraday-cup/RGEA combination.

The PBEA was well suited for neutral energy analysis, since energy discrimination was performed downstream from the ionizer. Although dc PBEA operation worked well for ion detection, two problems hindered its use for detecting neutral particles. First, the QMS ionizer efficiency was only about 0.05%,<sup>17</sup> resulting in a neutral signal per unit flux, which was a factor of 2000 times smaller than the ion signal. Second, at these low signal levels, a mass-independent background dominated the neutral signal. This background signal was present due to imperfect beam collimation in the PBEA, which allowed unionized fast neutrals to pass through the quadrupole rods and strike the particle detector. Since these fast neutrals were unaffected by the pole bias, the signal-to-noise ratio of the system was greatly increased by modulating the pole bias at 10 Hz and using lock-in detection. Energy analysis was obtained by fixing the maximum bias voltage at a level that rejected all of the ions and varying the modulation peak-to-valley amplitude. The shape of the modulated pole bias curve in Fig. 3 for ions, again indicates a sharp cutoff.

The QMS signal versus pole bias curves contained artifacts due to focusing effects in the RGEA, the small acceptance angle of the QMS, and the degraded response of the QMS to energetic particles. Thus, an energy distribution

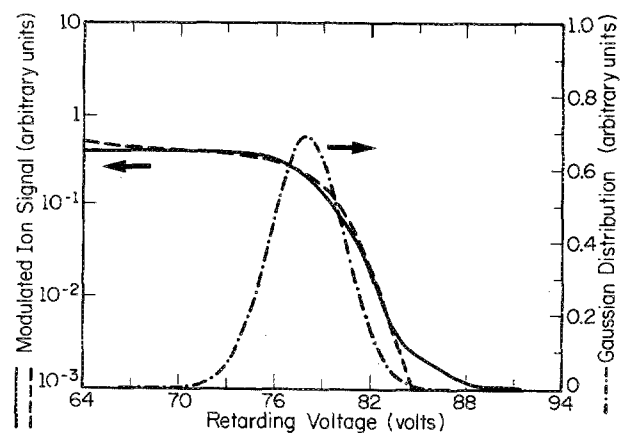


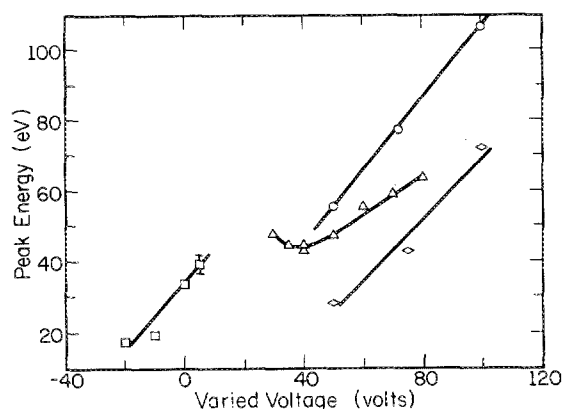
FIG. 4. The cut-off region of the QMS/modulated pole bias curve of Fig. 3 and the integrated Gaussian fit. The corresponding Gaussian distribution is also shown. The fit indicated a peak energy of 78 eV and a characteristic distribution width of 2.3 eV. Experimental (—), fit (---), and Gaussian (-·-·).

could not be obtained by differentiating these curves. These effects also will present a problem if more than one distribution is present, or if a single distribution is skewed to lower energies. Under such conditions, information about the lower energy species will be lost, and only results on the high energy portion of the distribution can be deduced. As a consequence, only the signal near the cutoff was used for curve fitting to obtain energy distributions. Good fits were obtained to the raw Faraday-cup data using numerically integrated Gaussian distributions. Based on the similar curve shapes shown in Fig. 3, all analysis methods were fit by this technique to obtain distribution information. An example of a fit to the QMS/modulated PBEA curve of Fig. 3 is shown in Fig. 4. Also shown is the corresponding Gaussian distribution which has a peak energy of 78 eV and a characteristic width of 2.3 eV. Although the neutral species studied in this investigation did not necessarily have Gaussian distributions, the fits were used to identify the neutral peak energy.

## B. Energy analysis

The ion energy was only dependent on, and was always slightly higher than, the ion beam acceleration voltage,  $V_b$ . As demonstrated in the potential diagram of Fig. 1, the ions received an added acceleration after falling through the plasma potential  $V_p$ . Integrated Gaussians fits showed that the characteristic widths of the ion energy distributions were between 1 and 3 eV.

In contrast to the ion energy distribution data, the neutral energy distributions were dependent on the ion gun operating parameters, and were always lower than the ion energy at



Symbol	Species	Varied Voltage	Discharge Voltage (volts)	Beam Voltage (volts)	Grid Voltage (volts)
○	Ions	Beam	40	—	5
△	Neutrals	Discharge	—	75	0
◇	Neutrals	Beam	40	—	0
□	Neutrals	Grid	40	50	—

FIG. 5. The peak energy of  $N_2^+$  ions vs the beam voltage (○),  $N_2$  neutrals vs the discharge voltage (△),  $N_2$  neutrals vs the beam voltage (◇), and  $N_2$  neutrals vs the grid voltage (□) created in a  $N_2$  discharge. Pressure = 1 mTorr,  $I_{\text{discharge}} = 50$  mA. The lines have been drawn as a visual aid.

a given  $V_b$  value. As shown in Fig. 5, the neutral energy increased with the discharge, beam, and grid voltages. Furthermore, the energy was independent of both the total gas pressure, which was varied between 0.5 and 1.5 mTorr, and the discharge current, which was varied between 50 and 500 mA. The characteristic widths of the neutral energy distributions ranged from 1.5 to 5 V, and were slightly larger than those of the ions.

These results can be explained if the neutralization process was charge-exchange occurring as the ions traverse the distance from the gun to the sampling orifice. Referring to Fig. 1, when charge transfer occurred in region A, the neutrals were formed with little kinetic energy and became part of the thermal background gas. Charge transfer in region B, the sheath regions of the grid, would result in energetic neutrals with an energy spread ranging from thermal up to  $e(V_b + V_p - V_g)$ , an energy that can be greater than that of the ions. The energy of fast neutrals produced in region C depends on the space charge potential of the positive unneutralized ion beam ( $V_{sp}$ ).

If it is assumed that the beam is composed of a long cylinder of positive charge, 2 cm in diameter, with 50 eV of kinetic energy, and a charge density of  $2.6 \times 10^{-11}$  C/cm<sup>3</sup> (determined with the current probe), then Gauss's law shows the potential is 72 V between the outside and the center of the beam. Furthermore, the corresponding electric field will be  $1.4 \times 10^2$  V/cm, causing an ion from the beam edge to move only 1.4 cm in the transverse beam direction after the traveling 20 cm. Such space charge potentials can account for the observed neutral energies, which are given by  $e(V_b + V_p - V_{sp})$ . Changes in the discharge, grid, and beam voltages not only change the total beam current, but also affect how the beam is focused, both resulting in a change in charge density and correspondingly in  $V_{sp}$ . It was observed that increasing the discharge voltage increased the ion beam charge density. The effect of the beam and grid voltages on the charge density were not investigated.

The large energy spread associated with charge exchange in region B was not observed. Even though the pressure near the sheath region of the grid may be up to an order of magnitude higher than the background pressure, the sheath distance, and thus the length over which charge-exchange takes place, is only on the order of 1 mm.<sup>1</sup> If scattering of both the energetic ion and neutral species out the beam is ignored, it can be shown that the fast neutral flux from region C will be at least 13 times greater than from region B if the beam travels 20 cm before striking the grounded wall. Scattering will tend to make this difference even larger.

## C. Neutral flux calibration

For the neutral flux calibration, the QMS signal height ( $S^0$ ), for a given thermal background pressure ( $P^{\text{QMS}}$ ), was used to determine the response ( $\beta$ ) of the QMS. This response was given by

$$\beta = 2 * S^0 / (P^{\text{QMS}} * 3.5 \times 10^{16}) \text{ V cm}^3/\text{atom}, \quad (1)$$

where  $P^{\text{QMS}}$ , measured in Torr, was monitored by an ion gauge whose signal had been corrected for the ionization efficiency of the gas used. The factor of 2 is an estimate which

which accounts for molecules with velocities in the correct direction to be accelerated into the QMS mass filter, since the background gas has a random velocity distribution. It was assumed that  $\beta$  also held for energetic particles, since thermal and energetic neutrals both had velocities much smaller than the ionizing electrons. As seen in Fig. 3, as the pole bias on the QMS was increased, the signal actually falls slightly. When the pole bias is within approximately 10–20 eV of the cut-off edge, a fast neutral will pass through the QMS rods at the same velocity as a thermal neutral that has been accelerated by the QMS extraction potential. The fast neutral signal heights in these experiments were obtained by modulating the pole bias between 0 V and a potential large enough to obtain complete signal cutoff. Therefore,  $\beta$  for the fast neutrals may be slightly larger than for the thermals.

With  $\beta$  determined and the pole bias modulated so that thermal neutrals were rejected, the energetic neutral flux was determined using the relationship

$$\Gamma = SvA/\beta, \quad (2)$$

where  $S$  was the energetic neutral signal,  $v$  was the velocity of the neutrals at their peak energy, and  $A$  was the ratio of the collimated beam volume to the total sensitive volume in the QMS ionizer. Using Eq. (2), it was estimated that the smallest detectable neutral flux using the PBEA was  $5 \times 10^{11}$  cm<sup>-2</sup> s<sup>-1</sup> with the ionization emission current at 10 mA.

The ion flux was calibrated with the current probe located in the main chamber midway between the gun and sampling orifice. If more than one type of ion species was detected, their charge state and the ratio of their QMS signals was used to determine the percentage of each present. Finally, the proportionality constant between the QMS and current probe signals was calculated. The measured energetic flux ranged from 1% to 8% of the ion flux at 0.5 mTorr. Losses in the ion flux due to charge exchange and scattering were not accounted for. These processes would increase the measured neutral to ion flux ratio.

#### IV. CONCLUSIONS

A QMS was shown to have energy analysis capabilities for both neutrals and ions when the quadrupole rods were bi-

ased with respect to ground. Modulation of the QMS pole bias greatly enhanced the signal-to-noise ratio of the system. This system was designed to evaluate *in situ* a wide range of deposition and etching techniques. For this study, the analyzer was used to characterize the species and energies of particles emitted from a single-grid, low-energy, Kaufman ion source. The ion energy was found to be equal to the sum of the beam and plasma potentials. The variation of the neutral energy distribution with the beam, discharge, and grid voltages was explained by a charge-exchange neutralization process.

#### ACKNOWLEDGMENTS

The authors wish to thank T. Slapikas of the Extrel Corp. and G. A. Tomasch for their technical assistance and Dr. J. Doyle for many fruitful discussions. This research was funded by EPRI under Contract No. RP2824-1, IBM, and the Joint Services Electronics Program.

<sup>1</sup>H. R. Kaufmann, J. J. Cuomo, and J. M. E. Harper, *J. Vac. Sci. Technol.* **21**, 725 (1982).

<sup>2</sup>N. P. Egorov and V. N. Komarov, *Sov. Phys. Tech. Phys.* **19**, 1100 (1975).

<sup>3</sup>T. Satake, T. Narusawa, O. Tsukakoshi, and S. Komiya, *Jpn. J. Appl. Phys.* **15**, 1359 (1976).

<sup>4</sup>L. P. Johnson, J. D. Morrison, and A. L. Wahrhaftig, *Int. J. Mass Spectrom. Ion Phys.* **26**, 1 (1978).

<sup>5</sup>A. R. Krauss and D. M. Gruen, *Appl. Phys.* **14**, 89 (1977).

<sup>6</sup>A. L. Gray and A. R. Date, *Analyst* **108**, 1033 (1983).

<sup>7</sup>J. A. Olivares and R. S. Houk, *Appl. Spectrosc.* **39**, 1070 (1985).

<sup>8</sup>D. E. Voss and S. A. Cohen, *Rev. Sci. Instrum.* **53**, 1969 (1982).

<sup>9</sup>R. B. Grant, *J. Vac. Sci. Technol. A* **5**, 2428 (1987).

<sup>10</sup>P. LeVaguerese and D. Pigache, *Rev. Phys. Appl.* **6**, 325 (1971).

<sup>11</sup>J. F. Smith and H. N. Southworth, *J. Phys. E* **14**, 952 (1980).

<sup>12</sup>H. R. Kaufman, *Fundamentals of Ion Source Operation* (Commonwealth Scientific Corp, 1984), p. 36.

<sup>13</sup>G. C. Elton, *J. Chem. Phys.* **15**, 455 (1947).

<sup>14</sup>S. N. Foner, *Adv. Atom. Mol. Phys.* **2**, 385 (1966).

<sup>15</sup>S. Stephanakis and W. H. Bennett, *Rev. Sci. Instrum.* **39**, 1714 (1968).

<sup>16</sup>J. A. Simpson, *Rev. Sci. Instrum.* **32**, 1283 (1961).

<sup>17</sup>W. Fite (private communication, 1989).